HIGH-FIDELITY SIMULATIONS OF ADVERSE PRESSURE GRADIENT FLOW OVER A ROUNDED STEP FOR TURBULENCE MODEL IMPROVEMENT VIA DATABASE GENERATION

***M. Rasquin*[1], *M. Boxho*[1], *T. Toulorge*[1], *K. Hillewaert*[1,2]**

[1] ***Centre de Recherche en Aéronautique (Cenaero), Belgium***
[2] ***Aerospace & Mechanics Department, Université de Liège (ULiège), Belgium***
michel.rasquin@cenaero.be

Abstract

It is widely acknowledged (Slotnick *et al*., 2014) that the prediction of turbulent flows in the presence of separation is one of the most significant challenges in fluid dynamics. Low cost simulation methods, such as Reynolds-Averaged Navier-Stokes (RANS) or even Wall-Modelled Large Eddy Simulations (WMLES) allow for an extensive exploration of the design space, but suffer from lower reliability especially for separated and secondary flows. Improving model reliability will therefore have a major impact on energy consumption, emission and noise of aircraft, cars, and ships due to significant improvements in design. The objective of this research is to generate a high-fidelity database on a representative and challenging configuration featuring flow separation. The resulting data can then be exploited to improve RANS and WMLES through machine learning and data-driven methodologies. The considered configuration is the HiFi-TURB DLR rounded step defined in Alaya, Grabe, and Eisfeld (2022) and Alaya and Grabe (2023). It has been designed to investigate the effect of an adverse pressure gradient on a turbulent boundary layer, which is relevant for many industrial flows. It features a separation bubble of which the start and extent are highly dependent on the correct capture of turbulent momentum transfer upstream.

1 Introduction

The HiFi-TURB DLR rounded step benchmark, developed within the European project HiFi-TURB (grant agreement no. 814837), is inspired by NASA's Axisymmetric Afterbody geometry proposed by Disotell and Rumsey (2017). This experimental configuration was designed to study flow separation over afterbodies, a phenomenon of critical relevance to the aerospace industry. A planar variant of the ramp was later investigated experimentally by (Simmons, Thomas, & Corke, 2018) at higher Reynolds numbers, underlining the interest in such configurations. From a numerical perspective, predicting flow separation remains particularly challenging for lower-fidelity turbulence models such as RANS and Wall-Modelled LES (WMLES). These ramp geometries therefore provide a discriminating benchmark for assessing turbulence model performance in near- and post-separation regimes.

2 Case Definition

The HiFi-TURB DLR rounded step features a planar design extruded in the spanwise direction, as illustrated in Figure 1, extracted from Alaya *et al*. (2022). The geometry comprises three main sections: an upstream flat plate section, the curved-step section, and a downstream flat plate section. The parametric geometry definition for the curved step sections is derived from Disotell and Rumsey (2017) and is further detailed for the proposed planar geometry in Alaya and Grabe (2023). To investigate different separation regimes, three ramp step heights of identical length is proposed, representing incipient, medium, and full separation. In all cases, the Reynolds number based on the step length is $Re_L = 433761$, whereas the Reynolds number Re_H based on the step height H varies with geometry, taking values of 78490, 98113, and 118768 respectively. In this work, the incipient separation case is considered.

A quasi-incompressible Mach number $Ma = 0.13455$ and a Prandlt number $Pr = 0.72$ are also imposed. The ratio between the step length L and step height H is set to $L/H = 5.5263$ for the incipient case. The target boundary layer at a reference point located 3.5H upstream the step is defined by $Re_\tau = \frac{\rho u_\tau \delta_{99}}{\mu} = 700$, where ρ is a reference density taken at the inlet, u_τ is the friction velocity and δ_{99}, the boundary layer height.

3 Numerical Approach

The numerical simulations in this study are performed using Argo, a high-order Discontinuous Galerkin Method (DGM) flow solver developed at Cenaero (Hillewaert, 2013; Carton de Wiart, Hillewaert, Bricteux, & Winckelmans, 2015). DGM combines the high accuracy of the finite element method (FEM) on unstructured meshes with the conservation properties of the finite volume method (FVM), making it

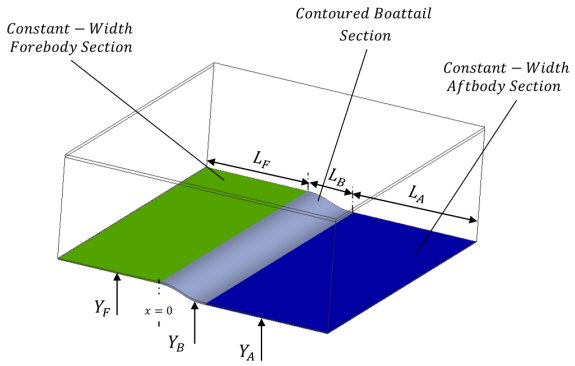

Figure 1: HiFi-TURB DLR rounded step geometry setup (Alaya *et al.*, 2022).

particularly effective for convection-dominated problems. ArgoDG discretizes the compressible Navier-Stokes equations and has been validated for Direct Numerical Simulations (DNS) of transitional flows in Carton de Wiart, Hillewaert, Duponcheel, and Winckelmans (2014). It has also been employed to investigate various complex flow regimes, including transonic flows in Hillewaert *et al.* (2016), transitional turbomachinery flows in Rasquin, Thomas, Bechlars, Franke, and Hillewaert (2023), and shock-dominated turbomachinery flows in Cagnone, Rasquin, Hillewaert, and Hiernaux (2017). This solver can handle arbitrary unstructured hybrid curved meshes, allowing elements of different topologies and accuracies. In this work, fourth-order polynomials are employed within the DGM framework to achieve fifth-order accuracy in the simulations. An implicit time integrator based on a Jacobian-free Newton-GMRES method, preconditioned with block-Jacobi, is utilized for the temporal discretization.

4 Numerical Setup

The flow separation at the step strongly depends on the characteristics of the incoming turbulent boundary layer. For that purpose, special attention is paid to the calibration of a reproducible procedure for generating a physically coherent developing turbulent boundary layer. The retained solution consists in prescribing first an incompressible laminar Blasius self-similar velocity profile (Schlichting, 1979) at the inlet, along with a uniform total temperature $T_{t,inlet} = 294.21$ K. This Blasius profile is characterized by $Re_{x,inlet} = 650{,}000$. Then, a numerical tripping source term is applied near the wall close to the inlet to trigger the transition of the boundary layer on the flat plate upstream the step, as proposed in Schlatter and Örlü (2010, 2012). The length of the flat plate region upstream of the step was primarily determined using a precursor flat plate simulation and by calibrating the tripping source term to achieve the target Re_τ at a reference point upstream of the step.

A static pressure $P_{outlet} = 89{,}593.58$ Pa is prescribed at the outlet and corresponds to the static pressure deduced from the the total pressure $P_{t,inlet} = 90{,}734.11$ Pa and the Mach number $Ma = 0.13455$ at the inlet (Alaya & Grabe, 2023). A no-slip adiabatic wall condition is applied on the three main sections of the rounded step. A free-stream boundary condition is located at a distance of $180H$ in the normal direction from the wall to avoid blockage effects. Lateral boundaries are periodic and a spanwise extension of $3H$ is expected to be sufficient for the incipient configuration to provide decorrelated statistics in the spanwise direction. A $20H$ extension from the beginning of the step to the pressure outlet boundary is prescribed. A sponge layer near the outlet is finally activated to mitigate spurious oscillations and reflections at the boundaries of the computational domain.

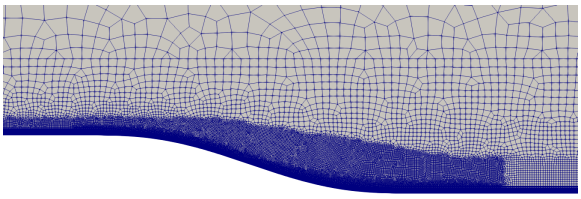

Figure 2: Side view of the mesh.

The mesh is illustrated in Figure 2 and is composed of 10.4 million fourth-order hexahedral elements, extruded into 188 layers in the spanwise direction. This results in roughly 1.3 billion degrees of freedom per equation (dof/eq) in total, with 125 Dof/eq per hexahedron. This mesh is partitioned in 65536 partitions and simulations are performed on the Lumi supercomputer hosted by CSC - IT Center For Science in Finland.

The effective mesh resolution at the wall, defined as the distance between successive Lagrange points, is shown in wall units in Figure 3. Upstream of the ramp, the boundary layer is resolved with $x^+ = 20$, $y^+ = 1$, and $z^+ = 13$ at the reference point. Slightly upstream of the ramp onset, the streamwise spacing is further reduced to $x^+ = 11$, yielding approximately isotropic quadrangles on the wall surface.

5 High-fidelity database

The goal of these high-fidelity simulations is to collect statistics for the improvement of both RANS and LES wall models using data-driven techniques and complement an existing database generated by Bassi, Colombo, and Massa (2023) from the University of Bergamo (UniBG) for the same case.

For RANS models, the simulations account for all terms arising from three distinct equations: the Favre-averaged Navier–Stokes, the Reynolds stress, and the kinetic energy dissipation equations. The Favre-averaged Navier–Stokes equations follow the formulation of Knight (1997). For the Reynolds stress equation, both the formulations of Knight (1997) and Gerolymos and Vallet (2001) are considered. The

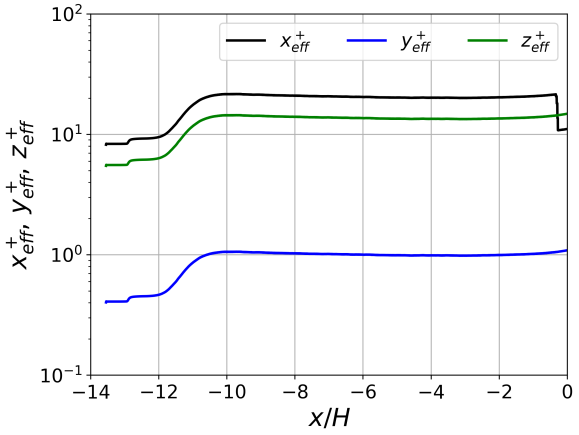

Figure 3: Effective mesh resolution at the wall upstream the ramp in wall units.

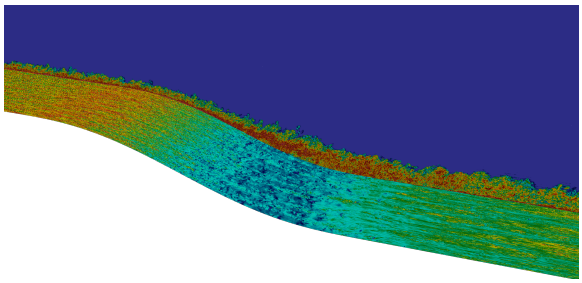

Figure 4: Instantaneous wall shear stress magnitude on the wall of the ramp, and vorticity field on the periodic plane for the incipient separation configuration of the HiFi-TURB DLR rounded step.

turbulent kinetic energy (TKE) equation is obtained by taking the trace of the Reynolds stress equations. Further details on the Favre-averaged Navier–Stokes and Reynolds stress formulations employed here are provided in Hillewaert and Rodi (2022). For the dissipation equation, we adopt the formulation of Kreuzinger, Friedrich, and Gatski (2006), which identifies the solenoidal component as the primary contributor in moderately compressible flows. These three governing equations are summarized in Rasquin *et al.* (2023). In addition, all intermediate quantities required for their computation, such as the strain-rate and rotation-rate tensors, are also collected.

To enhance the predictive capability of WMLES, instantaneous quantities are sampled at various heights above the step wall—including velocity, pressure, their gradients, and wall shear stress on the surface, following the strategy outlined in Boxho *et al.* (2022, 2025).

6 Results

The transient flow corresponding to the incipient separation configuration of the HiFi-TURB DLR rounded step has been simulated, and statistical quantities are currently being accumulated. Figure 4 illustrates this regime by showing the instantaneous wall-shear-stress magnitude on the surface together with the vorticity field on the periodic plane. This visualization was generated with a dedicated ParaView plugin capable of handling high-order polynomial solutions (Rasquin, Bauer, & Hillewaert, 2019).

Characterization of the upstream boundary layer

In general, flow separation is highly sensitive to the characteristics of the turbulent boundary layer (TBL) which develops upstream. Before performing the rounded-step simulations, a precursor turbulent boundary layer (TBL) simulation on a flat-plate was carried out to determine both the required upstream plate length and the strength of the tripping source term. The flat plate was then cut at the reference streamwise location where the target friction Reynolds number was achieved and connected to the remainder of the rounded step domain.

The evolution of the non-dimensional boundary-layer thickness, defined as $\delta^+ = \rho u_\tau \delta_{99}/\mu$, is of particular interest for characterizing the boundary layer. The definition of δ_{99} is however not straightforward in the presence of pressure gradients. Three different methods are employed to compute δ_{99} in this work. The first is the standard definition $u(y = \delta_{99}) = 0.99u_e$, which is highly sensitive to the far-field velocity (or external velocity) u_e. This velocity, together with δ_{99} can be fitted using the composite profile method originally proposed by Nickels (2004), although this approach is not well suited to TBL subject to pressure-gradients. To address this limitation, Vinuesa, Bobke, Örlü, and Schlatter (2016) proposed an iterative diagnostic-plot method, more robust for pressure-gradient flows, in which u_e and δ_{99} are determined such that $u'/(u\sqrt{H_{12}}) = 0.02$ and $u/u_e = 0.99$ at $y = \delta_{99}$. The third method defines δ_{99} from the integral of the vorticity norm:

$$\int_0^{\delta_{99}} \|\omega\| \mathrm{d}y = 0.99 \int_0^{\infty} \|\omega\| \mathrm{d}y, \qquad (1)$$

where ω denotes the vorticity.

To further characterize the TBL upstream of the rounded step, Figure 5 presents the evolution of the friction coefficient as a function of the Reynolds number based on the momentum thickness $Re_\theta = \rho u_e \theta/\mu$. The momentum thickness θ is defined as in Schlatter and Örlü (2010):

$$\theta(x) = \int_0^{\delta_{99}} \frac{u(x,y)}{u_e(x)} \left(1 - \frac{u(x,y)}{u_e(x)}\right) \mathrm{d}y \qquad (2)$$

where δ_{99} is evaluated using the diagnostic-plot method which provides the most robust estimate. In Figure 5 and subsequent figures, the symbol colors indicate the probe locations along the flat plate in the streamwise direction (blue near the domain inlet, red at the ramp start), while the red cross marks the TBL state at the reference point located at $-1.33R_{\max}$.

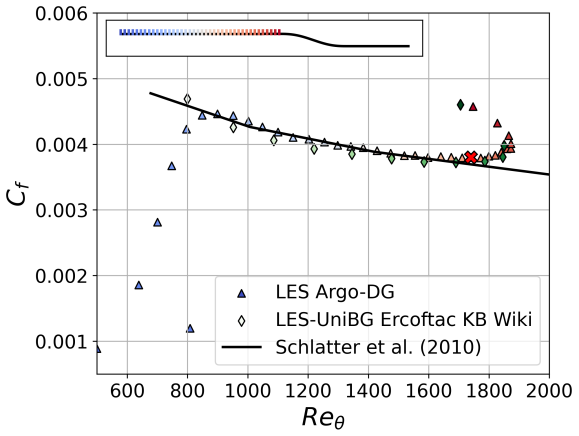

Figure 5: Evolution of the friction coefficient C_f along the flat plate upstream the rounded step.

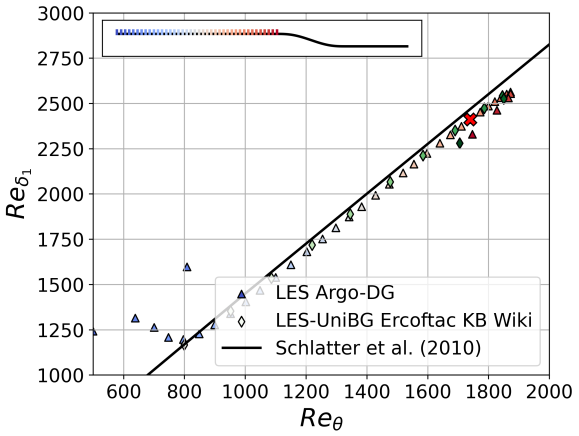

Figure 6: Evolution of the Reynolds number based on the displacement thickness along the flat plate upstream the step.

Up to the reference point, C_f agrees closely with the flat-plate zero-pressure-gradient DNS of Schlatter and Örlü (2010). Downstream of the reference location, the combined effect of the rounded step and the flow acceleration induced by the favorable pressure gradient upstream of the ramp leads to a sharp increase of C_f and a corresponding decrease of Re_θ relative to the reference DNS. The C_f data from the UniBG database confirm this observation and show good agreement with our results.

The evolution of the Reynolds number based on the TBL displacement thickness $Re_{\delta_1} = \rho u_e \delta_1 / \mu$ and the shape factor $H_{12} = \delta_1 / \theta$ is shown in Figures 6 and 7 respectively. The displacement thickness δ_1 is also defined as in Schlatter and Örlü (2010):

$$\delta_1(x) = \int_0^{\delta_{99}} \left(1 - \frac{u(x,y)}{u_e(x)}\right) \mathrm{d}y. \qquad (3)$$

Like in Figure 5, the displacement and momentum thicknesses are evaluated using δ_{99} obtained from the diagnostic-plot method. Re_{δ_1} and H_{12} agrees well with the DNS of Schlatter and Örlü (2010) up to the

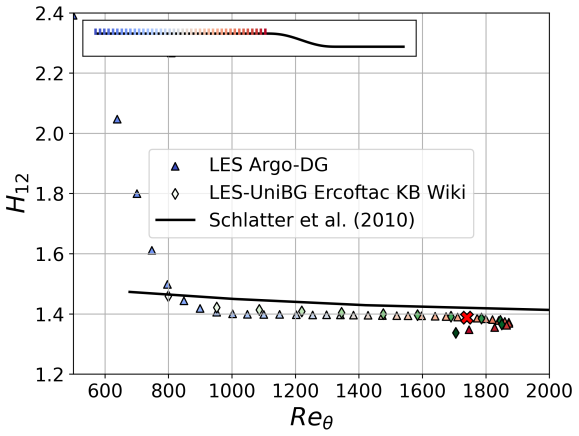

Figure 7: Evolution of the shape factor H_{12} along the flat plate upstream the step.

reference point, although a slight offset is observed between the DNS and the present results. The UniBG data are also in close agreement with our results and exhibit a similar offset relative to the DNS. Considering that the top boundary condition is located at a distance of $150H$ in the wall-normal direction to avoid blockage effects, this offset is attributed to the mild favorable pressure gradient upstream of the ramp.

Figure 8 shows the evolution of the TBL height in wall units $\delta^+ = \rho u_\tau \delta_{99} / \mu$, where δ_{99} is evaluated using the three methods introduced in this section: the standard approach based on a fixed value of u_e (circles), the diagnostic plot method (triangles), and the vorticity-integral method (squares). The momentum thickness is then computed following Equation 2 with the corresponding value of δ_{99}.

All methods predict a higher value of δ^+ on the flat plate upstream of the ramp compared to the reference DNS data, a trend also confirmed by the LES results from UniBG (diamond markers). The diagnostic plot method is applied to the LES-UniBG data to determine u_e, δ_{99}, and θ.

Although δ_{99} and θ are generally expected to decrease in a TBL subject to a favorable pressure gradient relative to a zero-pressure-gradient case due to flow acceleration, the larger value of δ^+ and Re_θ observed here are instead driven by higher friction velocity u_τ and external velocity u_e respectively.

Among the three methods for evaluating u_e, the standard definition with a fixed u_e produces a marked reduction in both δ^+ and Re_θ in Figure 8, and consequently in δ_{99} and θ. In contrast, the diagnostic-plot and vorticity-integral approaches adapt their external velocity, yielding larger values of δ_{99} and θ until the ramp effect becomes dominant and begins to influence these quantities.

At the reference point, the resulting $Re_\tau = 766$, $Re_\theta = 1711$ and $\delta_{99}/H = 0.185$, which is aligned with the target values defined in Alaya and Grabe (2023). At the start of the step located at $x/H = 0$,

$Re_\tau = 947$, $Re_\theta = 1747$ and $\delta_{99}/H = 0.208$.

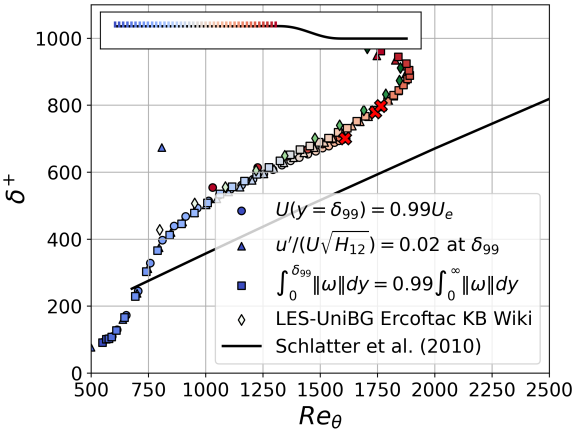

Figure 8: Evolution of the friction Reynolds number Re_τ along the flat plate upstream the rounded step.

7 Conclusions and perspectives

High-fidelity simulations of the incipient separation configuration of the HiFi-TURB DLR rounded step have been carried out with the high-order discontinuous Galerkin solver Argo. A detailed characterization of the incoming turbulent boundary layer has been presented, including friction coefficient, displacement and momentum thicknesses, as well as shape factor and friction Reynolds number. The analysis compared three methods for evaluating the boundary-layer thickness δ_{99} and showed that approaches which adapt the external velocity (diagnostic-plot and vorticity-integral methods) provide more consistent trends than the standard fixed-u_e definition for turbulent boundary layer subject to pressure gradients. The results agree well with the LES database from UniBG and highlight the sensitivity of δ^+ and Re_θ to the choice of external velocity definition and to the mild favorable pressure gradient upstream of the ramp.

Statistics and instantaneous quantities relevant to the improvement of RANS models and WMLES via data-driven and machine-learning approaches are currently being accumulated. Future work will provide detailed budgets of the turbulent kinetic energy and dissipation equations. The resulting datasets will be shared with the community through the ERCOFTAC Knowledge Base Wiki, complementing the existing UniBG database and fostering collaborative progress in turbulence modelling.

Acknowledgments

This work was supported until 2022 by the European Union's Horizon 2020 research and innovation programme HiFi-TURB (grant agreement No. 814837), and is supported more recently by the Horizon Europe programme ROSAS (grant agreement No. 101138319).

This work is also supported by he European Regional Development Fund (ERDF/FEDER) and the Walloon Region of Belgium through project 925 VirtualLab_Cenaero (programme 2021-2027).

The present research benefited from computational resources made available on the Tier-1 supercomputer of the Fédération Wallonie-Bruxelles, infrastructure funded by the Walloon Region under the grant agreement n°1117545.

We acknowledge PRACE for awarding the access to JUWELS hosted by GCS at FZJ, Germany. We acknowledge the EuroHPC Joint Undertaking for awarding this project access to the EuroHPC supercomputer LUMI, hosted by CSC (Finland) and the LUMI consortium, and the EuroHPC supercomputer VEGA hosted by IZUM (Slovenia) through EuroHPC Regular Access calls. We acknowledge EuroCC Belgium for awarding this project access to the LUMI supercomputer through the allocation Cenaero-HiFiDBTurb-T0331.

References

Alaya, E., & Grabe, C. (2023). ERCOFTAC knowledge base wiki: Ufr 3-36 hifi-turb-dlr rounded step. https://kbwiki.ercoftac.org/w/index.php/UFR_3-36_Test_Case. (Accessed: 2025-09-30)

Alaya, E., Grabe, C., & Eisfeld, B. (2022). Evolutionary algorithm applied to differential reynolds stress model for turbulent boundary layer subjected to an adverse pressure gradient. In AIAA Aviation 2022 Forum (p. 3337).

Bassi, F., Colombo, A., & Massa, F. C. (2023). ERCOFTAC knowledge base wiki: Dns 1-5 hifi-turb-dlr rounded step. https://kbwiki.ercoftac.org/w/index.php?title=DNS_1-5. (Accessed: 2025-09-30)

Boxho, M., Rasquin, M., Toulorge, T., Dergham, G., Winckelmans, G., & Hillewaert, K. (2022). Analysis of space-time correlations to support the development of wall-modeled LES. Flow, Turbulence and Combustion, 109(4), 1081–1109.

Boxho, M., Toulorge, T., Rasquin, M., Winckelmans, G., Dergham, G., & Hillewaert, K. (2025). Wall model based on a mixture density network to predict the wall shear stress distribution for turbulent separated flows. Flow, Turbulence and Combustion, 1–24.

Cagnone, J.-S., Rasquin, M., Hillewaert, K., & Hiernaux, S. (2017). Large eddy simulation of a low pressure compressor cascade at high incidence. In 12th european conference on turbomachinery fluid dynamics & thermodynamics.

Carton de Wiart, C., Hillewaert, K., Bricteux, L., & Winckelmans, G. (2015). Implicit LES of free and wall-bounded turbulent flows based on the discontinuous Galerkin/symmetric inte-

rior penalty method. International Journal for Numerical Methods in Fluids, 78. doi: 10.1002/fld.4021

Carton de Wiart, C., Hillewaert, K., Duponcheel, M., & Winckelmans, G. (2014). Assessment of a discontinuous Galerkin method for the simulation of vortical flows at high Reynolds number. International Journal for Numerical Methods in Fluids, 74(7), 469–493.

Disotell, K. J., & Rumsey, C. L. (2017). Development of an axisymmetric afterbody test case for turbulent flow separation validation (Tech. Rep. No. NASA/TM-2017-219680). NASA Langely Research Center.

Gerolymos, G., & Vallet, I. (2001). Wall-Normal-Free Reynolds-Stress Closure for Three-Dimensional Compressible Separated Flows. AIAA Journal, 39(10), 1833–1842.

Hillewaert, K. (2013). Development of the discontinuous Galerkin method for high-resolution, large scale CFD and acoustics in industrial geometries. Presses universitaires de Louvain.

Hillewaert, K., Cagnone, J., Murman, S., Garai, A., Lv, Y., & Ihme, M. (2016). Assessment of high-order DG methods for LES of compressible flows. In Proceedings of the center for turbulence research summer program.

Hillewaert, K., & Rodi, W. (2022). List of desirable and minimum quantities to be entered into the KB Wiki [Technical report]. ERCOFTAC KB WIKI (https://kbwiki-images.s3.amazonaws.com/8/80/List_of_desirable_and_minimum_quantities_to_be_entered_into_the_KB_Wiki.pdf).

Knight, D. D. (1997). Numerical simulation of compressible turbulent flows using the Reynolds-Averaged Navier-Stokes equations. In AGARD FDP Special Course on "Turbulence in Compressible Flows" (Vol. AGARD-R-819). von Karman Institute for Fluid Dynamics, Rhode-St-Genèse, Belgium.

Kreuzinger, J., Friedrich, R., & Gatski, T. (2006). Compressibility effects in the solenoidal dissipation rate equation: A priori assessment and modeling. International Journal of Heat and Fluid Flow, 27, 696–706.

Nickels, T. (2004). Inner scaling for wall-bounded flows subject to large pressure gradients. Journal of Fluid Mechanics, 521, 217–239. doi: 10.1017/S0022112004001788

Rasquin, M., Bauer, A., & Hillewaert, K. (2019). Scientific post hoc and in situ visualisation of high-order polynomial solutions from massively parallel simulations. International Journal of Computational Fluid Dynamics.

Rasquin, M., Thomas, J.-F., Bechlars, P., Franke, M., & Hillewaert, K. (2023). Direct numerical simulations of airfoil cascades for the improvement of turbulence models through database generation. In 15th european conference on turbomachinery fluid dynamics & thermodynamics.

Schlatter, P., & Örlü, R. (2010). Assessment of direct numerical simulation data of turbulent boundary layers. Journal of Fluid Mechanics, 659, 116–126.

Schlatter, P., & Örlü, R. (2012). Turbulent boundary layers at moderate reynolds numbers: inflow length and tripping effects. Journal of Fluid Mechanics, 710, 5–34.

Schlichting, H. (1979). Boundary-layer theory. Springer. doi: 10.1007/978-3-662-52919-5

Simmons, D. J., Thomas, F. O., & Corke, T. C. (2018). A smooth body, large-scale flow separation experiment. In 2018 AIAA Aerospace Sciences Meeting (p. 0572).

Slotnick, J. P., Khodadoust, A., Alonso, J., Darmofal, D., Gropp, W., Lurie, E., & Mavriplis, D. J. (2014). CFD vision 2030 study: A path to revolutionary computational aerosciences (Tech. Rep. No. CR–2014-218178). NASA.

Vinuesa, R., Bobke, A., Örlü, R., & Schlatter, P. (2016). On determining characteristic length scales in pressure-gradient turbulent boundary layers. Phys. Fluids, 28, 055101. doi: 10.1063/1.4947532